AI-driven discovery of synergistic drug combinations against pancreatic cancer

Mohsen Pourmousa[1+], Sankalp Jain[1+], Elena Barnaeva[1], Wengong Jin[2], Joshua Hochuli[3], Zina Itkin[1], Travis Maxfield[3], Cleber Melo-Filho[3], Andrew Thieme[3], Kelli Wilson[1], Carleen Klumpp-Thomas[1], Sam Michael[1], Noel Southall[1], Tommi Jaakkola[2], Eugene N. Muratov[3,4], Regina Barzilay[2], Alexander Tropsha[3,4], Marc Ferrer[1], Alexey V. Zakharov[1*].

[1] National Center for Advancing Translational Sciences (NCATS), National Institutes of Health, 9800 Medical Center Drive, Rockville, Maryland 20850, United States.

[2] Computer Science and Artificial Intelligence Laboratory, Massachusetts Institute of Technology, Cambridge, MA 02139, USA.

[3] Laboratory for Molecular Modeling, Division of Chemical Biology and Medicinal Chemistry, UNC Eshelman School of Pharmacy, University of North Carolina, Chapel Hill, NC, 27599, USA.

[4] Predictive, LLC. Raleigh, NC, 27614, USA.

+ authors contribute equally

* Address for correspondence: 9800 Medical Center Dr, Rockville, Maryland 20850, USA; Telephone: 301-480-9847; E-mail: alexey.zakharov@nih.gov.

Abstract

Treatment regimens, especially in cancer, often include more than one medicine in order to achieve durable outcomes. Identifying the optimal combination of treatments has historically been done through clinical trial and error. And for many conditions, such as pancreatic cancer, an optimal treatment protocol has remained elusive, and the best available treatment combinations provide only modest benefit. Recent developments have led to the application of both experimental screening approaches and *in silico* modeling methods to identify synergistic drug combinations and expand the therapeutic options for multiple diseases. Here we conduct a study to compare different predictive approaches for identifying new treatment combinations for pancreatic cancer using cell line growth as an initial proxy for clinical utility. NCATS performed screening involving 496 pairwise combinations of 32 antineoplastic drugs, tested against the PANC-1 human pancreatic carcinoma cell line in duplicates using a 10×10 matrix format. This dataset served as the basis for generating and training advanced AI/ML models focused on pancreatic cancer. Next, three independent groups (NCATS, UNC and MIT), though in a collaborative manner, utilized three different workflows with AL/ML approaches to discover new perspective drug combinations against pancreatic cancer among over 1.5 million drug combinations. As a result of this collaboration, 88 proposed combinations were tested in a cell-based assay; 53 of them were synergistic (hit rate ~60%). While all machine learning approaches demonstrate advances in the direction of predicting synergistic drug combinations, graph convolutional networks resulted in the best performance with a hit rate ~83%, and Random Forest delivered the highest precision of 65%. Interestingly, all utilized AL/ML methods among the three groups proposed different drug combinations with a small overlap of only two combos from 90. This study demonstrates the potential of a collaborative modeling approach for prioritizing drug combinations in large-scale screening campaigns, particularly when focusing on maximizing the efficacy of drugs known to exhibit synergy.

Introduction

Drug combinations have become standard therapy for numerous diseases including malaria, HIV, tuberculosis, and cancers [1–8]. Combination therapies can offer benefits such as enhanced efficacy, reduced toxicity, and avoiding the acquisition of monotherapy resistance [9–12]. In the case of pancreatic cancer, the prognosis in the past ten years has remained unchanged [13], and treatments have become ineffective [14–16] owing to growing resistance. Discovering anti-pancreatic cancer agents with high efficacy and low toxicity is crucial and constitutes one of the most challenging tasks for the scientific community working in oncology.

Effective drug combinations have been occasionally discovered in the clinic [17, 18], and there has also been an increase in preclinical experimental efforts to identify synergistic combinations reported in the literature [17, 19–22]. Employing combination therapy in the context of pancreatic cancer addresses the disease's heterogeneity and adaptive nature, leading to enhanced treatment efficacy and offering a promising strategy to overcome resistance mechanisms [23]. Though a few computational models have been reported in the literature recently [24–27], the extent of combination synergy in the context of pancreatic cancer remains largely unexplored.

Approved drugs have well-studied toxicity profiles and are readily available at scale for discovering new synergistic drug combinations. However, the sheer number of available and possible drug-like molecules [28] and an exponential number of their combinations make finding new therapeutic combinations highly inefficient by experimental means. High-throughput combinatorial screening is an established approach to identifying new synergistic drug combinations [29]; due to the exceedingly large number of unique chemical combinations, this approach is restrictive. In this context, *in silico* methods present an efficient complement to HTS and *in vitro* screening. [30–33].

One of the most popular computational drug discovery approaches, namely, Quantitative Structure-Activity Relationship (QSAR) modeling, employs statistical or machine learning approaches to establish and validate correlations between computed molecular features and experimentally measured biological activities of molecules [34–39]. This approach has been

widely applied in cancer drug discovery [24–27, 40, 41], using methods varying from simple linear [42–45] to non-linear machine learning methods, such as Neural Network (NN) [46], Support Vector Machine (SVM) [47] or Random Forest (RF) [48]. Most of the previous efforts covered the attempts to design novel monotherapies. However, recently, Cheng et al. [49] developed a biological network proximity measure using QSAR to predict drug synergy for hypertension and cancer. Other studies have utilized various machine learning techniques for synergy prediction [50–52], including deep learning approaches [53–55]. Preuer et al. [53] trained a deep neural network on a large oncology screen [56] and demonstrated the advantage of deep learning over standard machine learning models such as RFs and SVMs.

In this study, we combined efforts from three independent groups representing the National Center for Advancing Translational Sciences (NCATS), The University of North Carolina at Chapel Hill (UNC), and the Massachusetts Institute of Technology (MIT) to utilize different AI/ML methodologies to discover new prospective drug combinations against pancreatic cancer. To enable computational modeling studies, the NCATS team performed cell-based assays against pancreatic cancer, screening 1912 single agent compounds as well as assessing the most active 32 compounds (determined by IC_{50} and curve response class) for binary combinations using a 10 × 10 matrix format. Each team trained their models independently using 496 drug combinations in the training set with measured synergy effects on pancreatic cancer cell lines (see below for details of data generation) and predicted the top 30 synergistic combinations from 1.5 million possible combinations. Interestingly, among the proposed combinations from the three groups, there was almost no overlap (only two combos from 90), which emphasizes the importance of different AI/ML approaches. A cumulative selection of 88 drug combinations were then tested in a cell-based assay. This experimental validation resulted in 53 synergistic active combinations (out of 88 nominations; hit rate ~60%). We found that the graph convolutional method provided the best performance, with the hit rate ~83% and Random Forest showed the best precision result of 65%. In our opinion, there are several important conclusions of this study. First, and most importantly, it provides a successful example of using modern ML approaches to advance the experimental discovery of novel drug combinations for pancreatic cancer and, potentially, many other diseases. Second, it provides an interesting case study for benchmarking several common ML approaches differing in their complexity in a carefully designed prospective investigation. Finally, it outlines

the power of collaborative research using complementary but distinct ML methods in ensuring the highest experimental hit rate in computer-aided drug discovery.

Methods

Data generation

We used NCATS' in-house compound collection MIPE4 which consists of nearly 2,000 antineoplastic compounds with diverse and redundant mechanisms of action (MoA), and includes approved drugs, phases I−III investigational drugs, and pre-clinical molecules. The screening of this library and all following *in vitro* experiments were performed with continuous tumor-cell line from a human carcinoma of the exocrine pancreas (PANC-1) that is often used as a model for this highly aggressive type of pancreatic cancer.

The initial screening of MIPE4 library was performed in a duplicated single-agent dose-response manner (11 serial dilutions 1:3 in the range of [46uM – 0.78nM]. For this assay, PANC-1 cells were grown in DMEM media with 10% FBS and 1% antibiotics mix. The day of the experiment, they were harvested with 0.25% Trypsin for 5min, spun down and seeded as a cell suspension in growth media 500 cells/5ul/well. The cell density was experimentally selected based on efficient proliferation rate of cells for the period of 72 hours. Cells were plated onto white tissue culture-treated 1536-well Aurora plates (Brooks Automation, Chelmsford, MA) with MultiDrop Combi dispenser (Thermo Scientific, Logan, UT), and allowed to attach overnight at 37°C, 5% CO_2. Next, 23nl/well of compound solutions in DMSO were added to cells with a pintool transfer (Kalypsis, San Diego, CA). As the positive control, we used "no cells" column which would be equal to 100% killing capacity of a compound (IC_{100}), and DMSO was used as a vehicle neutral control (IC_0). The cells were stimulated with compounds or DMSO for 72 hours at 37°C, 5% CO_2, 95% humidity. For detection, we used CellTiter-Glo® Luminescent Cell Viability Assay (Promega, G7573) an ATP-based detection method of viable cells. This assay applies the properties of a thermostable firefly luciferase to generate a stable "glow-type" luminescent signal which could be measured within minutes when added directly to cell culture.

At the end of 72-hour stimulation period, 5ul/well of CellTiter-Glo® reagent was added to plates with BioRAPTR FRD dispenser. The plates were incubated at ambient temperature for 10 min and then the luminescent signal was read on ViewLux plate reader (PerkinElmer, Waltham, MA) with 3 sec exposure time.

From this MIPE4 library, the most active 32 molecules were selected based on their IC_{50} and curve response class (CRC) for further matrix combinations. They were run in "all versus all" combinations, totaling 496 unique pairwise combinations, as 10x10 matrices/blocks where two compounds were applied in nine 1:2 serial dilutions. The concentration range for each compound was selected individually to arrange their IC_{50} roughly in the middle of that range. Each block had a DMSO control (IC_0), as well as Bortezomib, a well-known cancer drug, as the positive control (IC_{100}). Each block was tested in duplicate.

To perform the matrix screening, the compounds mixtures were pre-dispensed to empty 1536-well white solid bottom plates with Echo 650 acoustic liquid handler (Beckman Coulter), 20nl/well each. Then, the plates were dispensed with PANC-1 cell suspension at 500 cells/5ul media density and placed in a tissue-culture incubator (5%CO_2, 37ºC, 95% humidity). CellTiter-Glo® reagent was added to wells 72 hours later for detection as described above.

Compounds standardization

Chemical structures of molecules in the training and test mixtures were standardized and curated following our canonical data curation practices using ChemAxon Standardizer version 20.9 [57, 58]. Briefly, salts and solvents were stripped from all compounds followed by removal of counterions, large organic compounds (Da ≥ 2000), mixtures, and inorganic compounds. Specific chemotypes such as aromatic, nitro groups, sulfo groups, tautomers, and protonation state were standardized using ChemAxon Standardizer software (https://chemaxon.com/).

Synergy Calculation

The degree of combination synergy (or antagonism) is quantified by comparing the observed compound combination response against the expected response, calculated using a reference model that assumes no interaction between compounds. The commonly-used reference models include the highest single agent (HSA) [59], Bliss [60], Loewe [61] and Zero interaction potency (ZIP) model [62]. In this study, different synergy metrics such as gamma (γ), beta, and Excess HSA were analyzed to measure the degree of reproducibility of duplicated combinations.

Computational Modeling Approach 1: NCATS

For machine learning, the molecular structures can be represented as numerical feature vectors, or molecular descriptors [63]. We employed several features and their concatenations to benchmark different machine learning methods. Each combination had two compounds and therefore two feature vectors were averaged to yield a single feature vector per combination. Avalon1024, Avalon2048, Morgan1024, and Morgan2048 fingerprints and RDKit descriptors (https://rdkit.org) were generated using python RDKit package. Additionally, an in-house Python 3.7.7 was used to generate biological descriptors from NCATS predictor (https://predictor.ncats.io/) [64]. Mechanisms of action were turned into feature vectors as follows: There were 821 unique mechanisms of action for the original 1784 PANC1 screening compounds. Each mechanism of action was encoded as an element in a vector of length 821, and the presence or absence of a mechanism of action for each combination was represented by 1 and 0, respectively. For instance, a combination with two distinct mechanisms of action would be encoded as a vector that has two elements set to 1 and the rest of them set to 0.

Random forest (RF) classification and regression [65, 66], eXtreme Gradient Boosting (XGBoost) [67], and deep neural network (DNN) [68] were used for benchmarking machine learning algorithm. Area under the curve (AUC) of the receiver operating characteristic (ROC) curve measured the performance of the classification models. XGBoost learning rates were tuned to be 0.01. DNN consisted of a sequential model with three hidden layers. The main parameters were optimized sequentially as follows: learning rate=0.0001, optimizer=Adam, batch size=128,

epochs=70. The number of neurons in hidden layers were tuned in a nested hyper parameter scheme with 700, 1000, and 2000 neurons in the first layer, 500 and 700 neurons in the second layer, and 200 and 300 neurons in the third layer.

Cross-validation scheme for training the model was one-compound-out [69]. This approach involves excluding one compound from each fold so that the fold has all the combinations except those containing that compound. As 32 compounds constituted the combinations (or training data), a total of 32 folds were performed within this scheme. The cross validation of the nested hyperparameter tuning in DNN split each 32 folds into three smaller folds.

Consensus modeling in general outperformed individual QSAR models [70, 71]. In this study, two approaches were taken to find consensus models: i) averaging the probabilities of individual models and ii) finding the majority vote from individual models. When finding the consensus model between classification and regression, the regression values were converted to pseudo-probabilities after scaling them to 0 to 1 and subtracting the scaled value from 1.

Computational Modeling Approach 2: UNC

General

RDKit descriptors and Morgan Fingerprints for both training set compounds and virtual screening library were calculated using the RDKit package in Python. Simplex descriptors [72, 73] were calculated with the HiT QSAR program [72]. Machine learning models were developed using the Python packages scikit-learn and PyTorch (for neural networks). Scikit-learn models used the default hyperparameters. All models were trained as classifiers (using binary labels) but produced a "confidence score" by different means. These "confidence scores" were averaged during consensus prediction calculation. Since the Simplex descriptors are computationally expensive [74], to calculate consensus predictions on the full test set, only the descriptor-based models with RDKit descriptors and Morgan Fingerprint were run to calculate consensus predictions on the full test set. Subsequently, the top 2,000 scoring combinations were evaluated with the Simplex-based models and the models with IC_{50} data.

Mechanism of Action selections

The training set columns 'MOA 1' & 'MOA 2' are aggregated and sorted, to form one MOA pair per row [one row per 496 unique drug pairs in training set]. Matrix rows are then grouped by unique MOA pairs. Counts of the number of rows from the original training set included, and the means for the 'label' [activity binary] column, were calculated for each of the 280 unique MOA pairs present in the training set. MOA pairs with 3 or more representative drug pairs in the training set, and a mean 'label' value greater than or equal to 0.66, were classified as the 24 most synergistic MOA pairs occurring in the training set. Chemotext [75], ROBOKOP [76]and knowledge graph mining [77] were used to identify and refine the MOAs of test compounds. Virtual screening of the test set [1.6M unique drug pairs], to remove drug pairs which do not represent any of the above 24 MOA pairs, yielded a subset of 888 unique drug pairs prioritized for selection by MOA model.

Pure descriptor models

A total of 15 model types trained purely on gamma binary labels were developed for use in consensus. Two descriptor types (RDKit descriptors and Morgan Fingerprint) were calculated for individual compounds in training mixtures and composited by either element-wise average or sum at every position in the descriptor. A third descriptor type, Simplex[72, 73], was calculated for the training mixtures, and did not require composition. Each of these descriptor/composition pairs was used as input for neural network, random forest, and gradient boosting models. To calculate a consensus, the prediction of every model for every descriptor was averaged. This resulted in three consensus models, each corresponding to a different descriptor.

Descriptor and IC$_{50}$ models

Two models were developed incorporating compound IC$_{50}$ data: a graph convolutional model and a neural network model based on Simplex descriptors. To develop the graph model, standardized SMILES strings for each of the constituent compounds were converted into graphs (adjacency matrices and node feature matrices) using the OpenChem software package [78]. A combined

mixture graph was created by taking the direct sum of individual adjacency matrices and the concatenation of node feature matrices. This combined graph was passed through a graph convolutional network resulting in a latent representation of the mixture graph, to which the respective Log IC_{50} values of each component compound were concatenated. The resulting representation was passed further through a neural network, and a classification score was produced as the final output.

For the neural network model, mixture Simplex descriptors were first produced and then cleaned, removing the highly correlated simplexes. The resulting Simplex descriptors were passed through several layers of a neural network, after which the Log IC_{50} values of each component compound were appended to the mixture representation. Like the graph model, the resulting representation was used as an input to the neural network model, and a classification score was produced as output. Each model was defined as above up to a set of hyperparameters (number of layers, size of each layer, learning rate, number of training epochs, etc.). To find optimal hyperparameters for each model, a specific mixture-oriented external validation was performed on several models. For a wide range of hyperparameter values, only insignificant differences were observed between models. Therefore, within this range, the final models were chosen for computational efficiency.

Computational Modeling Approach 3: ComboNet

MIT's ComboNet [79] approach utilizes a graph convolutional network that embeds a molecule into a continuous feature vector. This vector is learned automatically through the single-agent and combination data rather than hand-crafted. When trained on the single-agent data, the model takes a molecule as input and predicts whether it will inhibit cancer cell growth (binary label). When trained on the combination data, the model first takes a combination (A, B) as input and predicts the inhibition score c(AB) of this combination. Then it predicts their single-agent activity s(A) and s(B) and computes its expected inhibition score under bliss independence assumption: s(AB) = s(A) + s(B) - s(A)s(B). Finally, it quantifies the synergy score of combination (A, B) as c(AB) - s(AB). In addition to pancreatic cancer (PANC-1), our model is trained on 40 different cell lines collected from NCI-60 (single-agent data) [80]and NCI ALMANAC (combination data) [29]. Following a multi-task training scheme, our model is trained on 47K single-agent and 4K

combination data points in total, which is much larger than the PANC-1 data. To evaluate our approach, we split the pancreatic cancer combination dataset into training (80%), validation (10%) and test sets (10%).

Importantly, in this adaptation of ComboNet, we omitted drug-target interaction data, a deviation from the initial design [79], as it did not enhance the model's predictive accuracy.

Results and Discussion

Figure 1 provides an overview of the computational workflow adopted in this study. Three different modeling approaches were used to nominate 90 compounds, which result in a total of 4005 combinations, for further experimental validation.
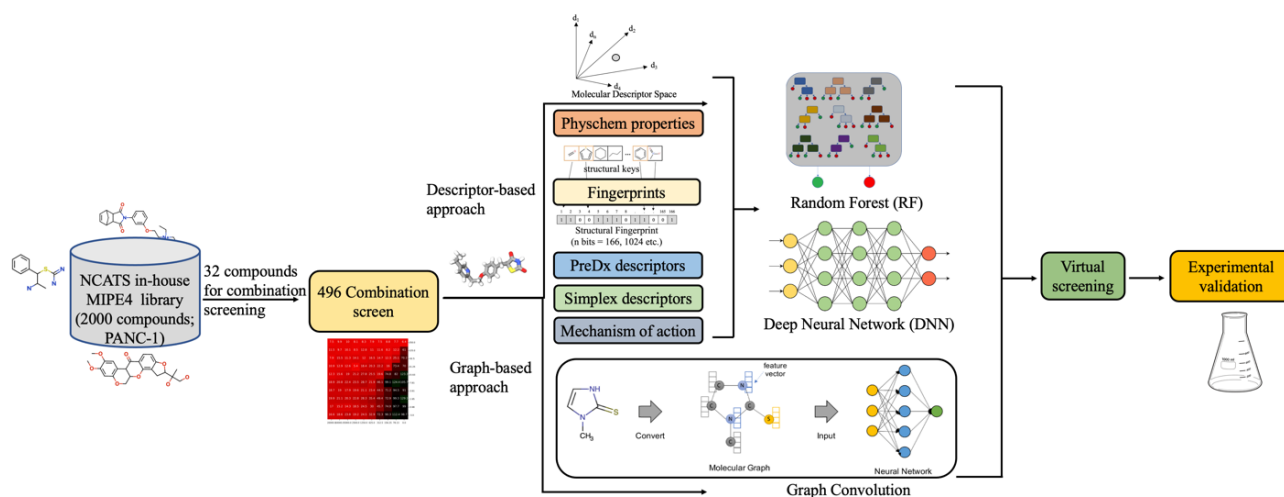
Figure 1: Computational workflow of the virtual screening strategy used in this study.

Data Overview

First, we performed the analysis of the PANC-1 training dataset. Figure 2 shows activity distribution of the 32 compounds in single-agent dose response curves used for modeling. The IC_{50} values range between 2 nM and 3 mM, which points out that the dataset is diverse in terms of the activity values. Next, all possible pairwise combinations of 32 compounds were plated and

screened in duplicates in 10×10 matrix format utilizing the PANC-1 cell line assay for generation of representative modeling set. We further analyzed the reproducibility of assay results and the best metrics to identify synergistic drug combinations. For this, we calculated the Pearson correlation of the gamma scores, beta, and Excess HSA. The correlation of gamma scores of duplicates was higher than the other two metrics (Figure 3, Supplementary Figure S1), confirming a great reproducibility of utilized assay system and matrix screening technology. Hence, gamma was used as the synergy metric with a cutoff of 0.95 ($\gamma \leq 0.95$ as synergistic and $\gamma > 0.95$ as non-synergistic or antagonist) [81]. The gamma scores were averaged for each duplicate resulting in one synergy value for each unique combination.
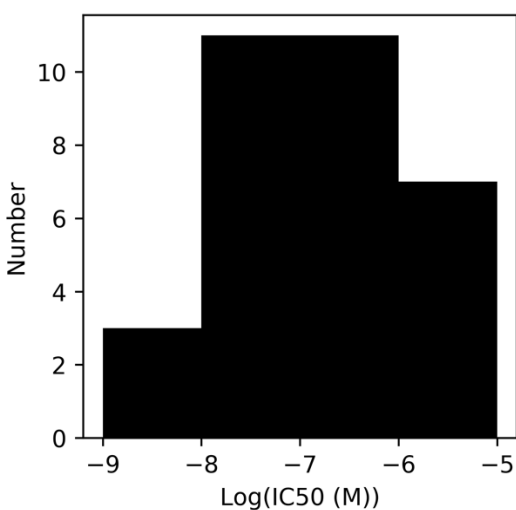

Figure 2: Variation of activity of 32 compounds in single-agent dose−response curves. Log(IC$_{50}$) varies between -8.7 to -5.5 ($\approx$ 2 nm−3 mM). These potent compounds constitute 496 combinations (all vs. all) used in this study.
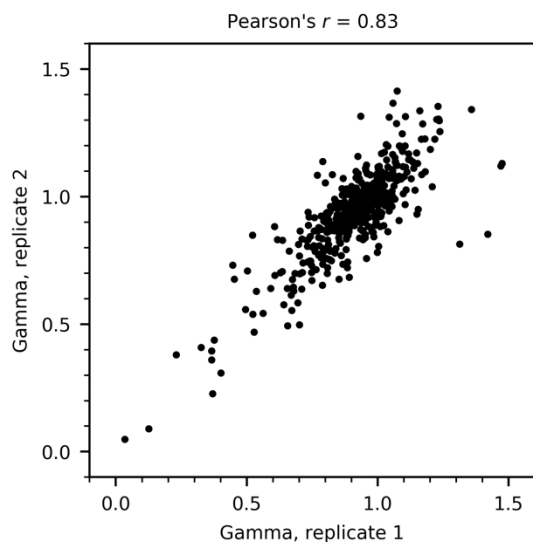
Figure 3: Reproducibility of combination experiments as measured by synergy metric. Gamma values of 496 combinations in two replicates have a Pearson's coefficient of 0.83. Combinations with Gamma < 0.95 are considered synergistic. Similar plots for other synergy metrics are in Supplementary Fig. S1.

A total of 496 combinations along with their corresponding scores were used as the training data. The original library of 1784 compounds, after omitting the 32 compounds, was used to generate 1,533,876 (all possible) pairwise combinations that serves as the virtual data set to predict prospectively and select new synergistic combination for further biological validation. Three modeling approaches were then pursued by three independent research groups and each approach provided a ranked list of top 30 synergistic combinations from the generated virtual set.

Modeling results

NCATS

Detailed model statistics on the training set and the test set are provided in Supplementary Table S1. All the models with different descriptors combination (as outlined in the method section) showed AUC values close to or above 75% for both training set and test datasets. Using a 2048-bit fingerprint resulted in improved model performance; in comparison to 1024-bit fingerprints and/or RDKit descriptors. Combining descriptors did not provide any performance improvement.

Overall, all three machine learning methods (RF, XGBoost and DNN) demonstrated fairly similar performance to different descriptor types. Combining RF classification and regression models based on Avalon2048 resulted in the highest AUC of 0.78±0.09 (Figure 4). This model was used to predict top 30 combinations (based on prediction score) from the virtual set comprising 1,591,724 combinations.
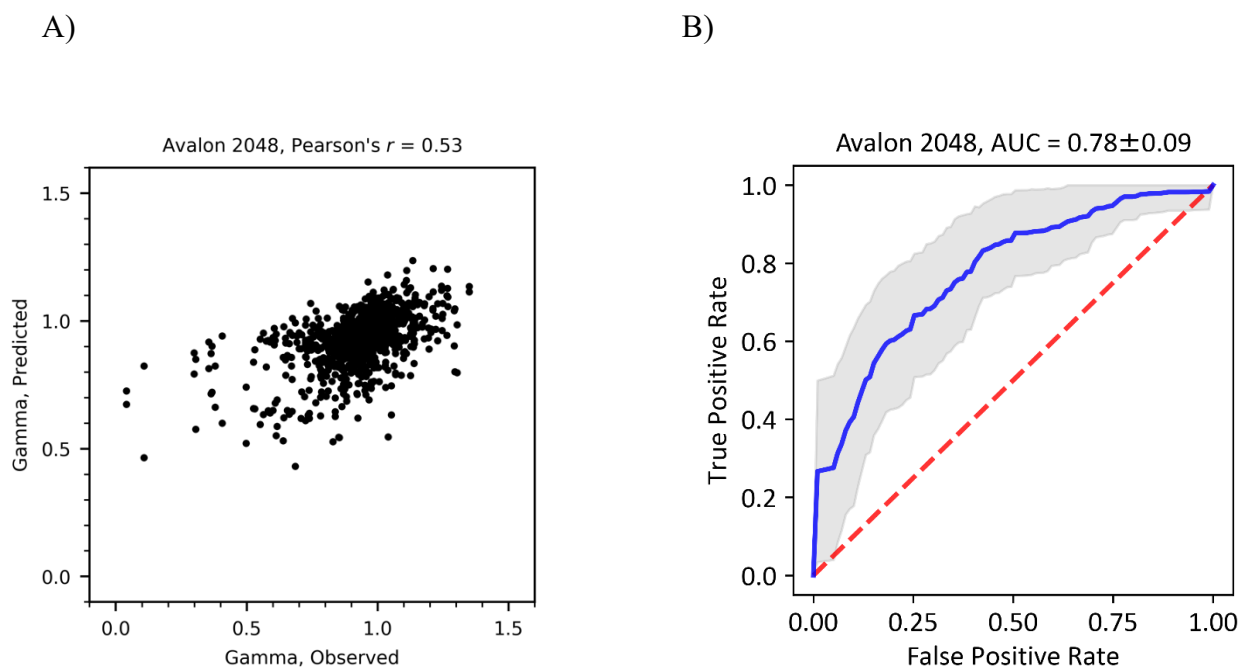
A)

B)

Figure 4: Random forest regression and classification models. Training set included 496 combinations constituted from 32 drugs (all vs. all). Cross validation strategy was one-compound-out, hence 32 folds. Average of Avalon 2048 fingerprints of each pair of drugs was used as the feature vector of combination. A) Regression models of Gamma of 32 folds are plotted on top of each other (Pearson's coefficient = 0.52). B) Classification model yields 32 ROC curves (not shown for clarity) with average AUC and standard deviation of 0.78 ± 0.09. Blue line, average ROC curve; grey area, ± 1 standard deviation; red line, random prediction; Gamma ≤ 0.95, synergistic; Gamma > 0.95, non-synergistic. Similar plots for Morgan 2048 and RDKit descriptors are in Supplementary Figures S2 and S3.

UNC

Model validation statistics for all evaluated models are reported in Supplementary Table S2. We applied two validation strategies: "compounds out" validation [82] and "everything out" validation [83]. For the "compounds out" validation strategy (evaluating on combinations containing one training compound and one non-training compound) most models produced a correct classification rate (or balanced accuracy) between 0.6 and 0.65 and had a positive predictive value (PPV)

between 0.6 and 0.7. For the "everything out" validation strategy (evaluating on combinations containing no training compounds), most models produced a CCR between 0.5 and 0.55, and a PPV between 0.5 and 0.6. This difference in results between validation strategies matches the expectation of "everything out" being a more challenging modeling task. For both validation strategies, y-randomization produced validation statistics consistent with random predictions.

Models using experimental IC_{50} values as part of chemical representation did not appear to have significantly better performance than models which omit them. Among the descriptor-based models, descriptor composition strategies (either averaging or summing columns) performed similarly.

Consensus model predictions were calculated as an average between the three descriptor consensus model predictions, and the two descriptors + IC_{50} individual model predictions. Only those combinations that included two active compounds and one training compound were considered for the first two tiers of nomination. Using the mechanism of action selection method (described in the methods section) and this criteria, 48 combinations were selected. Our first tier of nominations (n = 12) were those combinations from the set of 48 with a consensus prediction score > 0.7. The second tier of nominations (n = 12) were the highest scoring mixtures from pure descriptor model predictions. The third tier of nominations (n = 6) were combinations nominated by the mechanism of action criteria that were composed of two active compounds and no training compounds, then ranked by the models. The fourth tier of nominations (n = 12) were chosen from the set of 48 mechanism nominations with a model confidence between 0.6 and 0.7. The fifth tier of nominations were the next (n = 29) highest scoring mixtures from pure model predictions. The final tier of nominations were the next (n = 29) highest scoring mixtures from the mechanism of action selection with two active compounds and one training compound ranked by model confidence. The top 30 compounds were from the first three tiers, i.e., 12 combinations with mechanism of action + predicted score > 0.7 and 2 active compounds; 12 highest scoring combinations from remaining list with 2 active compounds; and then 6 combinations with mechanism of action, 2 active compounds, but no training compounds.
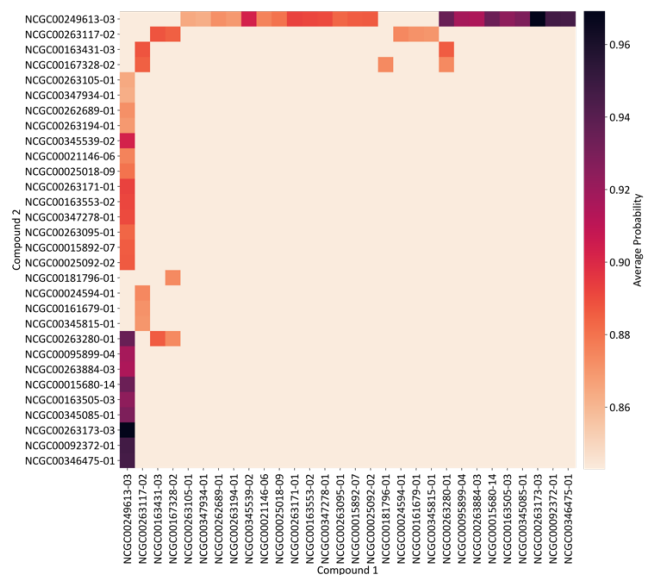
ComboNet

The results for the graph convolutional model are provided in Supplementary Table S3. The graph convolutional model achieved test AUC 0.840 +/- 0.036 (averaged under five different random splits; Supplementary Figure S4). This model was then applied to select the top 30 combinations.

Experimental validation

As described above, computational models were used to nominate a total of 90 compounds combinations for experimental validation. Interestingly, there were only 2 combinations that were common across the top 30 combinations which were suggested by both ComboNet and UNC. Thus, a total of 88 combinations were experimentally evaluated. Overall, the list of top 30 proposed compounds from respective institute for experimental testing were distinct. All combinations were tested in duplicates in 10×10 matrix format utilizing the PANC-1 cell line assay.

Considering the same cutoff for gamma (i.e., $\gamma \leq 0.95$ as synergistic), the models from all three institutes performed substantially well. The graph convolutional model from ComboNet was able to predict 25 out of 30 compound combinations correctly, thus providing the highest hit rate of 83%. The next best performing model was the RF model from NCATS, which is based on individual classification and regression RF models built using Avalon2048 descriptors. The NCATS models could identify 16 out of 30 combinations with a hit rate of 53%, followed by the models from UNC which provided a hit rate of 40%, predicting 12 out of 30 correctly. While both UNC and ComboNet used graph convolutional networks to predict drug synergy, ComboNet is trained on auxiliary data from NCI-ALMANAC which includes drug synergy data from multiple diseases (4000 data points). This could be a possible reason for the superior performance of ComboNet model. Interestingly, from both NCATS and UNC models, one compound demonstrated synergy with multiple other compounds. However, in the case of ComboNet, the list of synergistic combinations was diverse (Figure 5). During combination selection, MIT group also noticed that some compounds demonstrated synergy with many other compounds. To test a diverse set of drug combinations, MIT group selected the top five combinations for each compound, i.e., if a compound is predicted to be synergistic with many compounds, only five combinations are selected for testing. This resulted in a diverse selection of compounds.
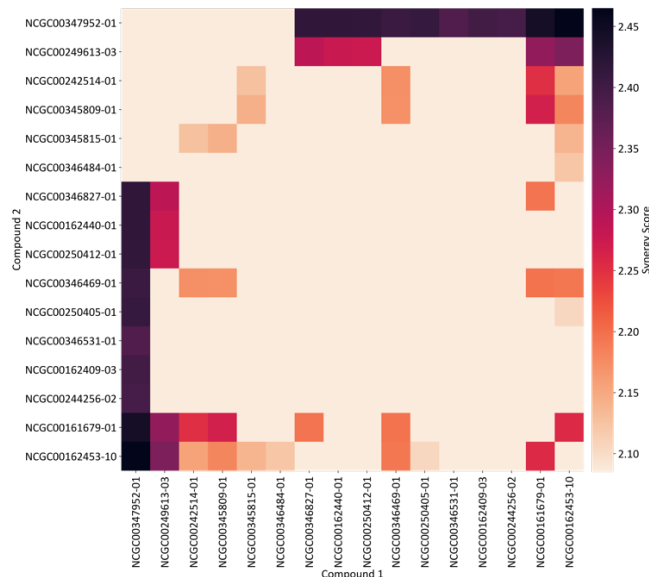
A) NCATS

B) UNC
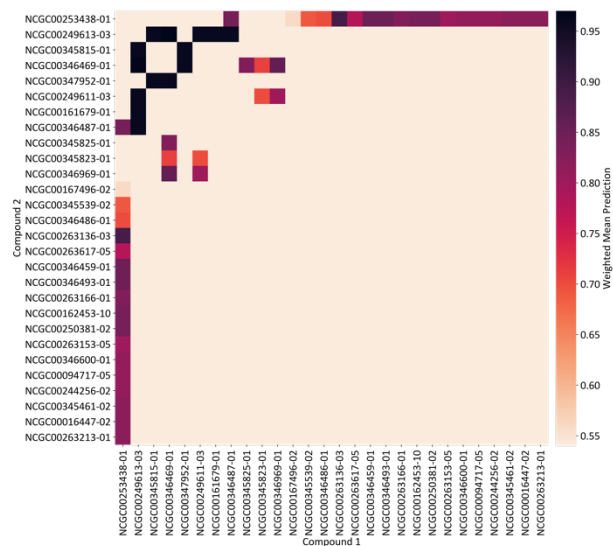
C) ComboNet

Figure 5: Heat map showing the selected compound combination by each institute. x-axis contact: compound 1, y-axis: compound 2; color scale: compound combination selection criteria adopted by respective institutes.

Finally, we retrospectively evaluated the final models from each institute for their ability to predict the 88 combinations selected for experimental testing (see Table 1, Figure 6). The NCATS models not only provide the highest balanced accuracy (BACC=0.59) but also yield the minimum number of false positives (FP), thus resulting in the highest precision of 0.65. Although ComboNet provided the highest AUC value (AUC = 0.78), it resulted in a high number of FP's. In terms of precision, the consensus of all three approaches did not result in any significant improvement. Thus, all three approaches yield considerably good results and could be recommended for the detection of synergistic drug combinations.

Table 1: Retrospective prediction of 88 nominated compounds from the respective final models from each institute

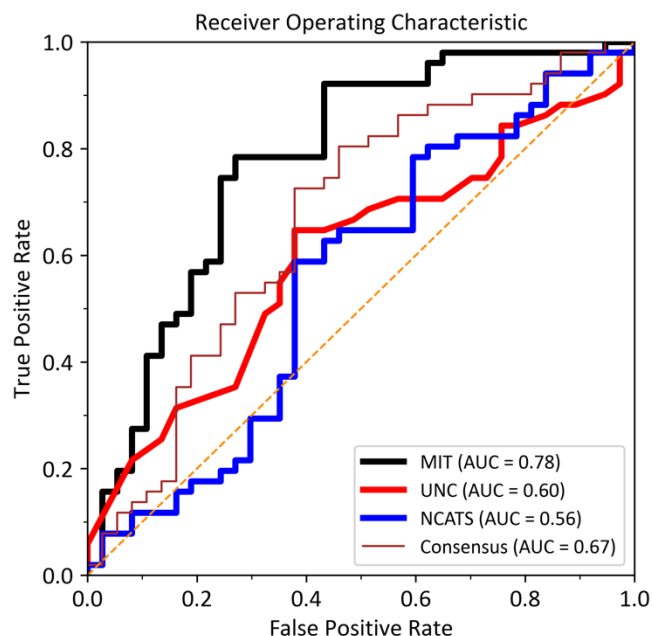|	TP	TN	FP	FN	Sens	Spec	Balanced Accuracy	AUC
NCATS	40	15	22	11	0.78	0.41	**0.59**	0.56
UNC	50	0	37	1	0.98	0.0	0.49	0.60
ComboNet	51	2	35	0	1.0	0.05	0.53	**0.78**
Consensus	51	2	35	0	1.0	0.05	0.53	0.67

Figure 6: Retrospectively prediction of 88 nominated compounds from the respective final models from each institute

 ORCID: https://orcid.org/0000-0003-2466-1711

Exploring the biological relevance of most synergistic combination against PANC-1

Among prospectively discovered new drug combinations both NSC-319726 and AZD-8055 showed good synergy with several drugs (Figure 7). Here we provide analysis of clinical prospective on these drugs.
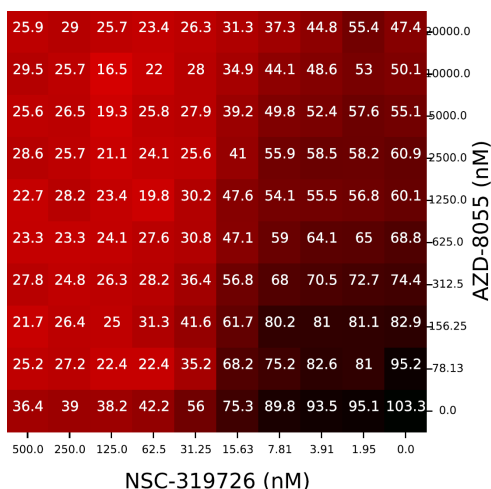

Figure 7: Matrix Blocks from NSC-319726 + AZD-8055 Drugs in PANC-1 Assay. The activity was normalized so that 100 corresponded to no cytotoxicity effect and 0 corresponded to full cytotoxicity effect.

NSC-319726 is a preclinical mutant p53 activator recognized as a critical process in the pancreatic tumor development [84, 85]. The clinical development of p53 activators, particularly MDM2 antagonists, and their relevance in pancreatic tumor development have been earlier reported [84, 86]. Notably, idasnutlin, an MDM2 antagonist, has entered phase III testing, signifying its advancement in clinical evaluation [87, 88]. Likewise, AZD-8055 is an mTOR (mechanistic target of rapamycin) inhibitor that has been investigated for its potential therapeutic value in various cancer types, including pancreatic tumors [89, 90]. The therapeutic exploitation of autophagy's role in pancreatic cancer has been explored through clinical trials using autophagy inhibitors, specifically chloroquine and hydroxychloroquine. However, these inhibitors have not shown significant clinical benefits in the metastatic stage of pancreatic cancer [91–93]. The lack of clinical benefits from autophagy inhibition may be due to the fact that clinically safe doses of drugs

do not inhibit autophagy enough to have a significant effect [80]. In pancreatic cancer, where KRAS is activated and p53 is disabled, cells can tolerate low levels of autophagy because the KRAS/BRAF/MAPK cascade sends inhibitory signals and p53 transcription is disabled, reducing autophagy protein levels. To achieve a clinically significant decrease in autophagy levels, inhibition of the KRAS/BRAF/MAPK cascade may be necessary, as this could have a synergistic effect with autophagy inhibition [91, 94]. The loss of p14ARF in pancreatic cancer cells may reduce their ability to induce autophagy, which could potentially make these cancer cells more sensitive to autophagy inhibition [84, 95]. Inhibition of autophagy in cancer cells is being explored as a therapeutic strategy, as it can disrupt their survival mechanisms and enhance the efficacy of other treatments [96].

In the clinical setting, the potential future for autophagy therapeutics lies in their combination with other targeted drugs, such as KRAS cascade inhibitors, specifically for well-defined molecular subtypes of pancreatic cancer that exhibit dependency on autophagy. This envisioned combination therapy approach would maximize the therapeutic impact by simultaneously targeting multiple key pathways involved in pancreatic cancer development and progression. Furthermore, in addition to the speculative perspective, the direct targeting of p53 activation holds promise in unlocking the full benefits of autophagy inhibition in the context of pancreatic cancer. However, further research and clinical studies are required to fully elucidate the synergistic effects and therapeutic potential of combining autophagy inhibition with p53 activation or other targeted therapies in pancreatic cancer.

Conclusion

Drugs synergy not only allows to maximize the efficacy but also helps achieve a desired therapeutic effect at lower doses of individual drugs, hence lowering the chances of side effects. Experimental assessment of drugs synergy is more expensive than examining single agents because, compared to the number of individual compounds, the total number of possible combinations is exponentially high. Therefore, AI/ML computational approaches such as network-based and structure-activity relationship methods can expedite identification and prioritization of synergistic combinations from large libraries of combinations. However, only a limited number of

studies reported prospective predictions of drug synergy, underlining the necessity and scope of exploring different computational approaches. Pancreatic cancer, characterized by complex molecular mechanisms involves multiple pathways in tumor development and progression and is resistant to conventional treatments, such as chemotherapy and radiation therapy. Thus, by synergistically targeting multiple critical pathways, combination approaches can have a greater impact on inhibiting tumor growth, inducing cell death, and suppressing metastasis. In this collaboration, we investigated three AI/ML workflows from three different independent groups for discovering drug synergistic combinations against pancreatic cancer. Overall, all the three approaches performed well and demonstrated a hit-rate ≥ 53% (experimental validation). While all machine learning approaches demonstrate advances in the direction of predicting synergistic drug combinations, graph convolutional networks resulted in the best performance with a hit rate ~83%, and Random Forest delivered the highest precision of 65%. Interestingly, all AL/ML models proposed different drug combinations with small overlap of only 2 combinations from 90, which emphasize the importance of utilizing different methods in early drug discovery over the most "predictive" ones. The synergy prediction workflow reported in this study is easily extendable for compound prioritization in large scale combination drug screenings and maximize the efficacy of drugs already known to induce synergy.

Acknowledgments

Conflict of interest

AT and ENM are co-founders of Predictive, LLC, which develops novel alternative methodologies and software for toxicity prediction.

References

1. Davies G, Boeree M, Hermann D, Hoelscher M (2019) Accelerating the transition of new tuberculosis drug combinations from Phase II to Phase III trials: New technologies and innovative designs. PLoS Med 16:e1002851. https://doi.org/10.1371/journal.pmed.1002851

2. Adam I, Ibrahim Y, Gasim GI (2018) Efficacy and safety of artemisinin-based combination therapy for uncomplicated Plasmodium falciparum malaria in Sudan: a systematic review and meta-analysis. Malar J 17:110. https://doi.org/10.1186/s12936-018-2265-x

3. Properzi M, Magro P, Castelli F, Quiros-Roldan E (2018) Dolutegravir-rilpivirine: first 2-drug regimen for HIV-positive adults. Expert Rev Anti Infect Ther 16:877–887. https://doi.org/10.1080/14787210.2018.1544491

4. Sun W, He S, Martínez-Romero C, et al (2017) Synergistic drug combination effectively blocks Ebola virus infection. Antiviral Res 137:165–172. https://doi.org/10.1016/j.antiviral.2016.11.017

5. Gotwals P, Cameron S, Cipolletta D, et al (2017) Prospects for combining targeted and conventional cancer therapy with immunotherapy. Nat Rev Cancer 17:286–301. https://doi.org/10.1038/nrc.2017.17

6. Mokhtari RB, Homayouni TS, Baluch N, et al (2017) Combination therapy in combating cancer. Oncotarget 8:38022–38043. https://doi.org/10.18632/oncotarget.16723

7. Tan X, Hu L, Luquette LJ, et al (2012) Systematic identification of synergistic drug pairs targeting HIV. Nat Biotechnol 30:1125–1130. https://doi.org/10.1038/nbt.2391

8. Yilancioglu K, Cokol M (2019) Design of high-order antibiotic combinations against M. tuberculosis by ranking and exclusion. Sci Rep 9:11876. https://doi.org/10.1038/s41598-019-48410-y

9. Sugahara KN, Teesalu T, Karmali PP, et al (2010) Coadministration of a Tumor-Penetrating Peptide Enhances the Efficacy of Cancer Drugs. Science 328:1031–1035. https://doi.org/10.1126/science.1183057

10. Holohan C, Van Schaeybroeck S, Longley DB, Johnston PG (2013) Cancer drug resistance: an evolving paradigm. Nat Rev Cancer 13:714–726. https://doi.org/10.1038/nrc3599

11. Crystal AS, Shaw AT, Sequist LV, et al (2014) Patient-derived models of acquired resistance can identify effective drug combinations for cancer. Science 346:1480–1486. https://doi.org/10.1126/science.1254721

12. Wood KB, Wood KC, Nishida S, Cluzel P (2014) Uncovering scaling laws to infer multidrug response of resistant microbes and cancer cells. Cell Rep 6:1073–1084. https://doi.org/10.1016/j.celrep.2014.02.007

13. Wang C, Yang A, Zhang B, et al (2014) PANC-1 Pancreatic Cancer Cell Growth Inhibited by Cucurmosin Alone and in Combination With an Epidermal Growth Factor Receptor–Targeted Drug. Pancreas 43:291–297. https://doi.org/10.1097/MPA.0000000000000087

14. Siegel RL, Miller KD, Jemal A (2015) Cancer statistics, 2015. CA Cancer J Clin 65:5–29. https://doi.org/10.3322/caac.21254

15. Bilimoria KY, Bentrem DJ, Ko CY, et al (2007) National failure to operate on early stage pancreatic cancer. Ann Surg 246:173–180. https://doi.org/10.1097/SLA.0b013e3180691579

16. Duong H-Q, Kim HJ, Kang HJ, et al (2012) ZSTK474, a PI3K inhibitor, suppresses proliferation and sensitizes human pancreatic adenocarcinoma cells to gemcitabine. Oncol Rep 27:182–188. https://doi.org/10.3892/or.2011.1503

17. Zoli W, Ricotti L, Tesei A, et al (2001) In vitro preclinical models for a rational design of chemotherapy combinations in human tumors. Crit Rev Oncol Hematol 37:69–82. https://doi.org/10.1016/s1040-8428(00)00110-4

18. Kurtz SE, Traer E, Martinez J, et al (2015) Identification of Effective Targeted Drug Combinations Using Functional Ex Vivo Screening of Primary Patient Specimens. Blood 126:865. https://doi.org/10.1182/blood.V126.23.865.865

19. Budman DR, Calabro A, Rosen L, Lesser M (2012) Identification of unique synergistic drug combinations associated with downexpression of survivin in a preclinical breast cancer model system. Anticancer Drugs 23:272–279. https://doi.org/10.1097/cad.0b013e32834ebda4

20. Kashif M, Andersson C, Hassan S, et al (2015) In vitro discovery of promising anti-cancer drug combinations using iterative maximisation of a therapeutic index. Sci Rep 5:14118. https://doi.org/10.1038/srep14118

21. Kischkel FC, Eich J, Meyer CI, et al (2017) New in vitro system to predict chemotherapeutic efficacy of drug combinations in fresh tumor samples. PeerJ 5:e3030. https://doi.org/10.7717/peerj.3030

22. Lieu CH, Tan A-C, Leong S, et al (2013) From Bench to Bedside: Lessons Learned in Translating Preclinical Studies in Cancer Drug Development. JNCI J Natl Cancer Inst 105:1441–1456. https://doi.org/10.1093/jnci/djt209

23. Lei F, Xi X, Batra SK, Bronich TK (2019) Combination Therapies and Drug Delivery Platforms in Combating Pancreatic Cancer. J Pharmacol Exp Ther 370:682–694. https://doi.org/10.1124/jpet.118.255786

24. Kumar R, Chaudhary K, Singla D, et al (2014) Designing of promiscuous inhibitors against pancreatic cancer cell lines. Sci Rep 4:4668. https://doi.org/10.1038/srep04668

25. Deokar H, Deokar M, Wang W, et al (2018) QSAR studies of new pyrido[3,4-b]indole derivatives as inhibitors of colon and pancreatic cancer cell proliferation. Med Chem Res 27:2466–2481. https://doi.org/10.1007/s00044-018-2250-5

26. Satbhaiya S, Chourasia OP (2015) Scaffold and cell line based approaches for QSAR studies on anticancer agents. RSC Adv 5:84810–84820. https://doi.org/10.1039/C5RA18295F

27. Singh H, Kumar R, Singh S, et al (2016) Prediction of anticancer molecules using hybrid model developed on molecules screened against NCI-60 cancer cell lines. BMC Cancer 16:77. https://doi.org/10.1186/s12885-016-2082-y

28. Polishchuk PG, Madzhidov TI, Varnek A (2013) Estimation of the size of drug-like chemical space based on GDB-17 data. J Comput Aided Mol Des 27:675–679. https://doi.org/10.1007/s10822-013-9672-4

29. Holbeck SL, Camalier R, Crowell JA, et al (2017) The National Cancer Institute ALMANAC: A Comprehensive Screening Resource for the Detection of Anticancer Drug Pairs with Enhanced Therapeutic Activity. Cancer Res 77:3564–3576. https://doi.org/10.1158/0008-5472.CAN-17-0489

30. Bulusu KC, Guha R, Mason DJ, et al (2016) Modelling of compound combination effects and applications to efficacy and toxicity: state-of-the-art, challenges and perspectives. Drug Discov Today 21:225–238. https://doi.org/10.1016/j.drudis.2015.09.003

31. Menden MP, Wang D, Mason MJ, et al (2019) Community assessment to advance computational prediction of cancer drug combinations in a pharmacogenomic screen. Nat Commun 10:2674. https://doi.org/10.1038/s41467-019-09799-2

32. Bobrowski T, Chen L, Eastman RT, et al (2021) Synergistic and Antagonistic Drug Combinations against SARS-CoV-2. Mol Ther 29:873–885. https://doi.org/10.1016/j.ymthe.2020.12.016

33. Muratov E, Zakharov A (2020) Viribus Unitis: Drug Combinations as a Treatment Against COVID-19. https://doi.org/10.26434/chemrxiv.12143355.v1

34. Ali M, Aittokallio T (2019) Machine learning and feature selection for drug response prediction in precision oncology applications. Biophys Rev 11:31–39. https://doi.org/10.1007/s12551-018-0446-z

35. Zakharov AV, Peach ML, Sitzmann M, et al (2012) Computational tools and resources for metabolism-related property predictions. 2. Application to prediction of half-life time in human liver microsomes. Future Med Chem 4:1933–1944. https://doi.org/10.4155/fmc.12.152

36. Jain S, Talley DC, Baljinnyam B, et al (2021) Hybrid In Silico Approach Reveals Novel Inhibitors of Multiple SARS-CoV-2 Variants. ACS Pharmacol Transl Sci 4:1675–1688. https://doi.org/10.1021/acsptsci.1c00176

37. Jain S, Norinder U, Escher SE, Zdrazil B (2021) Combining In Vivo Data with In Silico Predictions for Modeling Hepatic Steatosis by Using Stratified Bagging and Conformal Prediction. Chem Res Toxicol 34:656–668. https://doi.org/10.1021/acs.chemrestox.0c00511

38. Jain S, Ecker GF (2019) In Silico Approaches to Predict Drug-Transporter Interaction Profiles: Data Mining, Model Generation, and Link to Cholestasis. Methods Mol Biol Clifton NJ 1981:383–396. https://doi.org/10.1007/978-1-4939-9420-5_26

39. Abrams RPM, Yasgar A, Teramoto T, et al (2020) Therapeutic candidates for the Zika virus identified by a high-throughput screen for Zika protease inhibitors. Proc Natl Acad Sci U S A 117:31365–31375. https://doi.org/10.1073/pnas.2005463117

40. Mullen LMA, Duchowicz PR, Castro EA (2011) QSAR treatment on a new class of triphenylmethyl-containing compounds as potent anticancer agents. Chemom Intell Lab Syst 2:269–275. https://doi.org/10.1016/j.chemolab.2011.04.011

41. Chen J, Shen Y, Liao S, et al (2007) DFT-based QSAR study and molecular design of AHMA derivatives as potent anticancer agents. Int J Quantum Chem 107:1468–1478. https://doi.org/10.1002/qua.21285

42. Sabet R, Mohammadpour M, Sadeghi A, Fassihi A (2010) QSAR study of isatin analogues as in vitro anti-cancer agents. Eur J Med Chem 45:1113–1118. https://doi.org/10.1016/j.ejmech.2009.12.010

43. Speck-Planche A, Kleandrova VV, Luan F, Cordeiro MNDS (2011) Multi-target drug discovery in anti-cancer therapy: fragment-based approach toward the design of potent and versatile anti-prostate cancer agents. Bioorg Med Chem 19:6239–6244. https://doi.org/10.1016/j.bmc.2011.09.015

44. Pick A, Müller H, Mayer R, et al (2011) Structure-activity relationships of flavonoids as inhibitors of breast cancer resistance protein (BCRP). Bioorg Med Chem 19:2090–2102. https://doi.org/10.1016/j.bmc.2010.12.043

45. Speck-Planche A, Kleandrova VV, Luan F, Cordeiro MNDS (2012) Chemoinformatics in anti-cancer chemotherapy: multi-target QSAR model for the in silico discovery of anti-breast cancer agents. Eur J Pharm Sci Off J Eur Fed Pharm Sci 47:273–279. https://doi.org/10.1016/j.ejps.2012.04.012

46. González-Díaz H, Bonet I, Terán C, et al (2007) ANN-QSAR model for selection of anticancer leads from structurally heterogeneous series of compounds. Eur J Med Chem 42:580–585. https://doi.org/10.1016/j.ejmech.2006.11.016

47. Doucet J-P, Barbault F, Xia H, et al (2007) Nonlinear SVM Approaches to QSPR/QSAR Studies and Drug Design. Curr Comput - Aided Drug Des 3:263–289. https://doi.org/10.2174/157340907782799372

48. Singh H, Singh S, Singla D, et al (2015) QSAR based model for discriminating EGFR inhibitors and non-inhibitors using Random forest. Biol Direct 10:10. https://doi.org/10.1186/s13062-015-0046-9

49. Cheng F, Kovács IA, Barabási A-L (2019) Network-based prediction of drug combinations. Nat Commun 10:1197. https://doi.org/10.1038/s41467-019-09186-x

50. Li P, Huang C, Fu Y, et al (2015) Large-scale exploration and analysis of drug combinations. Bioinforma Oxf Engl 31:2007–2016. https://doi.org/10.1093/bioinformatics/btv080

51. Wildenhain J, Spitzer M, Dolma S, et al (2015) Prediction of Synergism from Chemical-Genetic Interactions by Machine Learning. Cell Syst 1:383–395. https://doi.org/10.1016/j.cels.2015.12.003

52. Li H, Li T, Quang D, Guan Y (2018) Network Propagation Predicts Drug Synergy in Cancers. Cancer Res 78:5446–5457. https://doi.org/10.1158/0008-5472.CAN-18-0740

53. Preuer K, Lewis RPI, Hochreiter S, et al (2018) DeepSynergy: predicting anti-cancer drug synergy with Deep Learning. Bioinforma Oxf Engl 34:1538–1546. https://doi.org/10.1093/bioinformatics/btx806

54. Xia F, Shukla M, Brettin T, et al (2018) Predicting tumor cell line response to drug pairs with deep learning. BMC Bioinformatics 19:486. https://doi.org/10.1186/s12859-018-2509-3

55. Sidorov P, Naulaerts S, Ariey-Bonnet J, et al (2019) Predicting Synergism of Cancer Drug Combinations Using NCI-ALMANAC Data. Front Chem 7:509. https://doi.org/10.3389/fchem.2019.00509

56. O'Neil J, Benita Y, Feldman I, et al (2016) An Unbiased Oncology Compound Screen to Identify Novel Combination Strategies. Mol Cancer Ther 15:1155–1162. https://doi.org/10.1158/1535-7163.MCT-15-0843

57. Fourches D, Muratov E, Tropsha A (2010) Trust, but verify: on the importance of chemical structure curation in cheminformatics and QSAR modeling research. J Chem Inf Model 50:1189–1204. https://doi.org/10.1021/ci100176x

58. Fourches D, Muratov E, Tropsha A (2016) Trust, but Verify II: A Practical Guide to Chemogenomics Data Curation. J Chem Inf Model 56:1243–1252. https://doi.org/10.1021/acs.jcim.6b00129

59. Berenbaum MC (1989) What is synergy? Pharmacol Rev 41:93–141

60. Bliss CI (1939) The Toxicity of Poisons Applied Jointly1. Ann Appl Biol 26:585–615. https://doi.org/10.1111/j.1744-7348.1939.tb06990.x

61. Loewe S (1953) The problem of synergism and antagonism of combined drugs. Arzneimittelforschung 3:285–290

62. Yadav B, Wennerberg K, Aittokallio T, Tang J (2015) Searching for Drug Synergy in Complex Dose-Response Landscapes Using an Interaction Potency Model. Comput Struct Biotechnol J 13:504–513. https://doi.org/10.1016/j.csbj.2015.09.001

63. Todeschini R, Consonni V (2008) Handbook of Molecular Descriptors. John Wiley & Sons

64. Zakharov AV, Zhao T, Nguyen D-T, et al (2019) Novel Consensus Architecture To Improve Performance of Large-Scale Multitask Deep Learning QSAR Models. J Chem Inf Model 59:4613–4624. https://doi.org/10.1021/acs.jcim.9b00526

65. Breiman L (2001) Random Forests. Mach Learn 45:5–32. https://doi.org/10.1023/A:1010933404324

66. Breiman L (1993) Classification and regression trees. Chapman & Hall, New York [u.a.

67. Chen T, Guestrin C (2016) XGBoost: A Scalable Tree Boosting System. In: Proceedings of the 22nd ACM SIGKDD International Conference on Knowledge Discovery and Data Mining. Association for Computing Machinery, New York, NY, USA, pp 785–794

68. LeCun Y, Bengio Y, Hinton G (2015) Deep learning. Nature 521:436–444. https://doi.org/10.1038/nature14539

69. Zakharov AV, Varlamova EV, Lagunin AA, et al (2016) QSAR Modeling and Prediction of Drug–Drug Interactions. Mol Pharm 13:545–556. https://doi.org/10.1021/acs.molpharmaceut.5b00762

70. Valsecchi C, Grisoni F, Consonni V, Ballabio D (2020) Consensus versus Individual QSARs in Classification: Comparison on a Large-Scale Case Study. J Chem Inf Model 60:1215–1223. https://doi.org/10.1021/acs.jcim.9b01057

71. Jain S, Siramshetty VB, Alves VM, et al (2021) Large-Scale Modeling of Multispecies Acute Toxicity End Points Using Consensus of Multitask Deep Learning Methods. J Chem Inf Model. https://doi.org/10.1021/acs.jcim.0c01164

72. Kuz'min VE, Artemenko AG, Muratov EN (2008) Hierarchical QSAR technology based on the Simplex representation of molecular structure. J Comput Aided Mol Des 22:403–421. https://doi.org/10.1007/s10822-008-9179-6

73. Kuz'min V, Artemenko A, Ognichenko L, et al (2021) Simplex representation of molecular structure as universal QSAR/QSPR tool. Struct Chem 32:1365–1392. https://doi.org/10.1007/s11224-021-01793-z

74. Kuz'min VE, Muratov EN, Artemenko AG, et al (2008) The effects of characteristics of substituents on toxicity of the nitroaromatics: HiT QSAR study. J Comput Aided Mol Des 22:747. https://doi.org/10.1007/s10822-008-9211-x

75. Capuzzi SJ, Thornton TE, Liu K, et al (2018) Chemotext: A Publicly Available Web Server for Mining Drug–Target–Disease Relationships in PubMed. J Chem Inf Model 58:212–218. https://doi.org/10.1021/acs.jcim.7b00589

76. Bizon C, Cox S, Balhoff J, et al (2019) ROBOKOP KG and KGB: Integrated Knowledge Graphs from Federated Sources. J Chem Inf Model 59:4968–4973. https://doi.org/10.1021/acs.jcim.9b00683

77. (2019) The Biomedical Data Translator Program: Conception, Culture, and Community. Clin Transl Sci 12:91–94. https://doi.org/10.1111/cts.12592

78. Korshunova M, Ginsburg B, Tropsha A, Isayev O (2021) OpenChem: A Deep Learning Toolkit for Computational Chemistry and Drug Design. J Chem Inf Model 61:7–13. https://doi.org/10.1021/acs.jcim.0c00971

79. Jin W, Stokes JM, Eastman RT, et al (2021) Deep learning identifies synergistic drug combinations for treating COVID-19. Proc Natl Acad Sci 118:e2105070118. https://doi.org/10.1073/pnas.2105070118

80. Shoemaker RH (2006) The NCI60 human tumour cell line anticancer drug screen. Nat Rev Cancer 6:813–823. https://doi.org/10.1038/nrc1951

81. Mathews Griner LA, Guha R, Shinn P, et al (2014) High-throughput combinatorial screening identifies drugs that cooperate with ibrutinib to kill activated B-cell-like diffuse large B-cell lymphoma cells. Proc Natl Acad Sci U S A 111:2349–2354. https://doi.org/10.1073/pnas.1311846111

82. Muratov EN, Varlamova EV, Artemenko AG, et al (2012) Existing and Developing Approaches for QSAR Analysis of Mixtures. Mol Inform 31:202–221. https://doi.org/10.1002/minf.201100129

83. Muratov E, Varlamova E, Kuz'min V, et al (2014) JSM Clinical Pharmaceutics " Everything Out " Validation Approach for Qsar Models of Chemical Mixtures. J Clin Pharm 1:1005

84. Voutsadakis IA (2021) Mutations of p53 associated with pancreatic cancer and therapeutic implications. Ann Hepato-Biliary-Pancreat Surg 25:315–327. https://doi.org/10.14701/ahbps.2021.25.3.315

85. Hassin O, Oren M (2023) Drugging p53 in cancer: one protein, many targets. Nat Rev Drug Discov 22:127–144. https://doi.org/10.1038/s41573-022-00571-8

86. Wang W, Qin J-J, Voruganti S, et al (2018) Discovery and characterization of dual inhibitors of MDM2 and NFAT1 for pancreatic cancer therapy. Cancer Res 78:5656–5667. https://doi.org/10.1158/0008-5472.CAN-17-3939

87. Khurana A, Shafer DA (2019) MDM2 antagonists as a novel treatment option for acute myeloid leukemia: perspectives on the therapeutic potential of idasanutlin (RG7388). OncoTargets Ther 12:2903–2910. https://doi.org/10.2147/OTT.S172315

88. A Study of Idasanutlin With Cytarabine Versus Cytarabine Plus Placebo in Participants With Relapsed or Refractory Acute Myeloid Leukemia (AML) - Full Text View - ClinicalTrials.gov. https://clinicaltrials.gov/ct2/show/NCT02545283. Accessed 27 Jun 2023

89. Ali ES, Mitra K, Akter S, et al (2022) Recent advances and limitations of mTOR inhibitors in the treatment of cancer. Cancer Cell Int 22:284. https://doi.org/10.1186/s12935-022-02706-8

90. Tao Z, Li T, Ma H, et al (2018) Autophagy suppresses self-renewal ability and tumorigenicity of glioma-initiating cells and promotes Notch1 degradation. Cell Death Dis 9:1063. https://doi.org/10.1038/s41419-018-0957-3

91. Xu J, Patel NH, Gewirtz DA (2020) Triangular Relationship between p53, Autophagy, and Chemotherapy Resistance. Int J Mol Sci 21:8991. https://doi.org/10.3390/ijms21238991

92. Wolpin BM, Rubinson DA, Wang X, et al (2014) Phase II and pharmacodynamic study of autophagy inhibition using hydroxychloroquine in patients with metastatic pancreatic adenocarcinoma. The Oncologist 19:637–638. https://doi.org/10.1634/theoncologist.2014-0086

93. Karasic TB, O'Hara MH, Loaiza-Bonilla A, et al (2019) Effect of Gemcitabine and nab-Paclitaxel With or Without Hydroxychloroquine on Patients With Advanced Pancreatic Cancer: A Phase 2 Randomized Clinical Trial. JAMA Oncol 5:993–998. https://doi.org/10.1001/jamaoncol.2019.0684

94. Bryant KL, Stalnecker CA, Zeitouni D, et al (2019) Combination of ERK and autophagy inhibition as a treatment approach for pancreatic cancer. Nat Med 25:628–640. https://doi.org/10.1038/s41591-019-0368-8

95. Balaburski GM, Hontz RD, Murphy ME (2010) p53 and ARF: unexpected players in autophagy. Trends Cell Biol 20:363–369. https://doi.org/10.1016/j.tcb.2010.02.007

96. Lim SM, Mohamad Hanif EA, Chin S-F (2021) Is targeting autophagy mechanism in cancer a good approach? The possible double-edge sword effect. Cell Biosci 11:56. https://doi.org/10.1186/s13578-021-00570-z